

Relativistic Hartree approach with exact treatment of vacuum polarization for finite nucleiAkihiro Haga,^{1,*} Setsuo Tamenaga,^{1,†} Hiroshi Toki,^{1,‡} and Yataro Horikawa^{2,§}¹*Research Center for Nuclear Physics (RCNP), Osaka University, Ibaraki, Osaka 567-0047, Japan*²*Department of Physics, Juntendo University, Inba-gun, Chiba 270-1695, Japan*

(Received 4 September 2004; published 27 December 2004)

We study the relativistic Hartree approach with an exact treatment of the vacuum polarization in the Walecka (σ - ω) model. The contribution from the vacuum polarization of the nucleon-antinucleon field to the source term of the meson fields is evaluated by performing the energy integrals of the Dirac Green function along the imaginary axis. With the present method of calculating the vacuum polarization in finite system, the total binding energies and charge radii of ^{16}O and ^{40}Ca can be reproduced. On the other hand, the level splittings in the single-particle level, in particular the spin-orbit splittings, are not described well because the inclusion of vacuum effect provides a large effective mass with small meson fields. We also show that the derivative expansion of the effective action is fairly useful for the estimation of the vacuum effect.

DOI: 10.1103/PhysRevC.70.064322

PACS number(s): 21.10.-k, 21.60.-n, 13.75.Cs

I. INTRODUCTION

It is well known that the relativistic field theory based on the hadrons, referred to as quantum hadrodynamics (QHD), has been very successful in describing the ground states of finite nuclei [1]. When the energy functional of the relativistic mean field (RMF) is fitted to nuclear saturation, the RMF model automatically produces an appropriate order of the spin-orbit splitting of nuclei, the spin-observables of the proton-nucleus scattering and the energy dependence of the proton-nucleus optical potential. In RMF, however, only positive-energy nucleons are taken into account in the calculation, in spite of the existence of solutions with negative energy, which is one of the interesting characters of the relativistic picture. The negative-energy states are observables in antinucleonic atoms. The bound levels of antinucleonic atoms are predicted to be much deeper than those of ordinary nucleon states since the magnitudes of the nucleon-scalar and nucleon-vector self-energies, which are very large, cancel each other to provide the usual binding energy in the nucleon sector, while they reinforce each other in the antinucleon sector (see Ref. [2] and references therein). It is important to study if this feature remains when we treat the negative-energy states explicitly in the QHD framework. Knowledge of the depth of antinucleon binding in the nucleus would be valuable in the search for the exotic collective antimatter production proposed by Greiner [3].

Recently, the gauge invariant nuclear-polarization calculation was carried out in the relativistic random-phase approximation (RRPA) based on the RMF theory. It was found that the RRPA eigenstates with negative energy have a significant role, since the transverse form factors of these states become considerably large [4]. If antinucleons are deeply bound, the transverse response function has a contribution

from the antinucleon states with an energy lower than twice the nucleon mass. In that case, electron-scattering or photo-absorption may confirm the large binding of the antinucleon. In order to investigate the antinucleon state in the QHD model, however, we are required to take into account the contribution of vacuum polarization of the nucleon-antinucleon field to the mean field for consistency. This means that the RMF model without vacuum contribution has to be extended to the full one-nucleon-loop approximation, which we refer to as the relativistic Hartree approximation (RHA).

The vacuum contributions and their effects on the bound states of positive energy were investigated by several authors within the local-density approximation and the derivative-expansion method [5–12]. After refitting the parameters of the model to the properties of spherical nuclei, it was found that the RHA calculation can reproduce the experimental data of the binding energies and the rms radii of nuclei as well as the RMF can. On the other hand, due to the decrease of the scalar and vector potentials by the feedback from the vacuum in the RHA calculation, the effective mass of nucleon becomes large and the binding energy of antinucleon small compared with the RMF.

Despite the finding of the importance of the vacuum effect, however, the exact evaluation of one-loop corrections in a finite nuclear system has never been performed. This is an exceedingly difficult task, since the exact treatment of vacuum polarization in finite nuclei requires the computation of not only the valence nucleon with positive energy but also an infinite number of negative-energy states. In this context, an excellent method has been developed in quantum electrodynamics (QED) [13,14]; the summation over eigenstates is replaced by an energy integral of the Dirac Green function along the imaginary axis in which the Green functions do not oscillate. With this approach, it is possible to perform the calculation much faster. Blunden carried out the exact RHA calculation of QHD in 1+1 dimensions and the calculation of quantum solitons model in 3+1 dimensions [15,16]. In the present paper we will apply this method, developed in the context of atomic physics, to the RHA calculation of QHD.

*Electronic address: haga@rcnp.osaka-u.ac.jp

†Electronic address: stame@rcnp.osaka-u.ac.jp

‡Electronic address: toki@rcnp.osaka-u.ac.jp

§Electronic address: horikawa@sakura.juntendo.ac.jp

This paper is organized as follows. In Sec. II A, we introduce the effective Lagrangian density used in this work and give the outline of the renormalization in the source term of meson fields. The method to obtain the renormalized vacuum densities is given in Sec. II B for the baryon density, and in Sec. II C for the scalar density. The details of the computational procedure for the calculation of the vacuum correction are described in Sec. III. In Sec. IV, the numerical results of the RHA calculation including vacuum corrections for baryon and scalar densities are presented for ^{16}O and ^{40}Ca and the effect of the vacuum on the properties of the nucleus is discussed. In Sec. V, we will also compare our rigorous method with the local-density approximation and the derivative expansion. Finally, we give a summary of our calculation in Sec. VI.

II. RELATIVISTIC HARTREE APPROACH IN FINITE NUCLEUS

A. Lagrangian density

The nucleus is described as a system of Dirac nucleons which interact in a relativistic covariant manner through the exchange of several mesons; the scalar meson (σ) produces a strong attraction, while the isoscalar vector meson (ω) produces a strong repulsion for the nucleon sector. In the present work, we employ a Lagrangian density including the photon (A), as well as the σ and ω mesons as

$$\begin{aligned} \mathcal{L}_N = & \bar{\psi}_N (i\gamma^\mu \partial_\mu - m_N) \psi_N + \frac{1}{2} \partial_\mu \sigma \partial^\mu \sigma - \frac{1}{2} m_\sigma^2 \sigma^2 - \frac{1}{3} g_2 \sigma^3 \\ & - \frac{1}{4} g_3 \sigma^4 - \frac{1}{4} (\partial_\mu \omega_\nu - \partial_\nu \omega_\mu)^2 + \frac{1}{2} m_\omega^2 \omega_\mu \omega^\mu \\ & - \frac{1}{4} (\partial_\mu A_\nu - \partial_\nu A_\mu)^2 - g_\sigma \bar{\psi}_N \sigma \psi_N - g_\omega \bar{\psi}_N \gamma_\mu \omega^\mu \psi_N \\ & - \frac{1}{2} e \bar{\psi}_N (1 + \tau_3) \gamma_\mu A^\mu \psi_N - \delta\mathcal{L}, \end{aligned} \quad (1)$$

where

$$\begin{aligned} \delta\mathcal{L} = & -\frac{1}{4} \zeta_\omega (\partial_\mu \omega_\nu - \partial_\nu \omega_\mu)^2 + \frac{1}{2} \zeta_\sigma \partial_\mu \sigma \partial^\mu \sigma + \alpha_1 \sigma + \frac{1}{2} \alpha_2 \sigma^2 \\ & + \frac{1}{3} \alpha_3 \sigma^3 + \frac{1}{4} \alpha_4 \sigma^4 \end{aligned} \quad (2)$$

denotes counterterms to renormalize the nucleon density which has a divergence from the vacuum. Since this Lagrangian density includes the nonlinear coupling terms for the σ meson, the one- σ -meson loop also can contribute to the nucleon density [9,11]. In the present paper, however, we neglect this contribution for the sake of simplicity. Assuming that the nuclear ground state is spherically symmetric, the Hartree basis consists of eigenfunctions of the following Dirac equation:

$$\begin{aligned} & \left[\gamma^0 \left(\epsilon_N - g_\omega \omega_0(\mathbf{r}) - \frac{1}{2} e (1 + \tau_3) A_0(\mathbf{r}) \right) + i\boldsymbol{\gamma} \cdot \boldsymbol{\nabla} \right. \\ & \left. - (m_N + g_\sigma \sigma(\mathbf{r})) \right] \psi_N(\mathbf{r}) = 0. \end{aligned} \quad (3)$$

The meson fields $\omega_0(\mathbf{r})$ and $\sigma(\mathbf{r})$ satisfy the Klein-Gordon equations:

$$(-\nabla^2 + m_\omega^2) \omega_0(\mathbf{r}) = g_\omega \rho_{\omega \text{ ren}}(\mathbf{r}), \quad (4)$$

$$(-\nabla^2 + m_\sigma^2) \sigma(\mathbf{r}) = -g_\sigma \rho_{\sigma \text{ ren}}(\mathbf{r}) - g_2 \sigma^2(\mathbf{r}) - g_3 \sigma^3(\mathbf{r}), \quad (5)$$

respectively. The renormalized baryon [$\rho_{\omega \text{ ren}}(\mathbf{r})$] and scalar [$\rho_{\sigma \text{ ren}}(\mathbf{r})$] densities are given by

$$\rho_{\omega \text{ ren}}(\mathbf{r}) = \int_C \frac{dz}{2\pi i} \text{Tr}[\gamma_0 G^H(\mathbf{r}, \mathbf{r}; z)] + (CT), \quad (6)$$

$$\rho_{\sigma \text{ ren}}(\mathbf{r}) = \int_C \frac{dz}{2\pi i} \text{Tr}[G^H(\mathbf{r}, \mathbf{r}; z)] + (CT), \quad (7)$$

where $G^H(\mathbf{r}, \mathbf{r}; z)$ is the single-particle Green function of the Hartree approximation with the potential terms of the Dirac equation (3). The z integrations are carried out along the modified Feynman contour which lies below the real axis up to the nuclear Fermi energy [13,14]. The divergences arising from these integrals are cancelled by the contributions from the counterterms denoted by CT. This procedure will be discussed in detail in Sec. II B and II C. The integral along the Feynman contour can be changed to an integral over the imaginary z axis, with additional pole contributions from the positive-energy states up to Fermi level. Thus, we may write the unrenormalized baryon and scalar densities as

$$\begin{aligned} & \int_C \frac{dz}{2\pi i} \text{Tr}[\gamma^0 G^H(\mathbf{r}, \mathbf{r}; z)] \\ & = \sum_{\epsilon_i > 0}^F \psi_i^\dagger(\mathbf{r}) \psi_i(\mathbf{r}) - \int_{-i\infty}^{+i\infty} \frac{dz}{2\pi i} \text{Tr}[\gamma^0 G_V^H(\mathbf{r}, \mathbf{r}; z)], \end{aligned} \quad (8)$$

$$\begin{aligned} & \int_C \frac{dz}{2\pi i} \text{Tr}[G^H(\mathbf{r}, \mathbf{r}; z)] \\ & = \sum_{\epsilon_i > 0}^F \bar{\psi}_i(\mathbf{r}) \psi_i(\mathbf{r}) + \int_{-i\infty}^{+i\infty} \frac{dz}{2\pi i} \text{Tr}[G_V^H(\mathbf{r}, \mathbf{r}; z)], \end{aligned} \quad (9)$$

respectively. Here, G_V^H is the vacuum part of the single-particle Green function of the relativistic Hartree approximation:

$$G^H(\mathbf{r}_1, \mathbf{r}_2; z) = G_D^H(\mathbf{r}_1, \mathbf{r}_2; z) + G_V^H(\mathbf{r}_1, \mathbf{r}_2; z), \quad (10)$$

$$G_D^H(\mathbf{r}_1, \mathbf{r}_2; z) = 2\pi i \sum_{\epsilon_i > 0}^F \delta(z - \epsilon_i) \psi_i(\mathbf{r}_1) \bar{\psi}_i(\mathbf{r}_2), \quad (11)$$

$$G_V^H(\mathbf{r}_1, \mathbf{r}_2; z) = \sum_{\epsilon_i > 0} \frac{\psi_i(\mathbf{r}_1) \bar{\psi}_i(\mathbf{r}_2)}{z - \epsilon_i + i\eta} + \sum_{\epsilon_i < 0} \frac{\psi_i(\mathbf{r}_1) \bar{\psi}_i(\mathbf{r}_2)}{z - \epsilon_i - i\eta}. \quad (12)$$

The numerical integration for G_V^H along the imaginary z axis can be carried out straightforwardly, since there are no poles in the integrand. Although the second terms of right-hand sides of Eqs. (8) and (9) have divergences, an expansion of the total vacuum correction in the coupling constants g_ω and g_σ of the meson fields verifies that all divergences are contained in the first order of g_ω for the baryon density, and are contained in terms up to the third order of g_σ for the scalar

density. In the following subsections, we show that these divergences are removed by taking the proper counterterms (2) into account.

B. Vacuum correction for the baryon density

In this subsection, we consider the vacuum correction for the baryon density. For the estimation of the vacuum correction, we will treat the proton and neutron on an equal footing, to save numerical effort. In order to deal with the unrenormalized density containing the divergence, we start with a perturbative expansion in ω and σ fields:

$$\begin{aligned} \int_{-i\infty}^{+i\infty} \frac{dz}{2\pi i} \text{Tr}[\gamma^0 G_V^H(\mathbf{r}, \mathbf{r}; z)] &= \int_{-i\infty}^{+i\infty} \frac{dz}{2\pi i} \text{Tr}[\gamma^0 G^0(\mathbf{r}, \mathbf{r}; z)] + \int_{-i\infty}^{+i\infty} \frac{dz}{2\pi i} \text{Tr} \left[\int d\mathbf{x} \gamma^0 G^0(\mathbf{r}, \mathbf{x}; z) g_\omega \gamma^0 \omega(\mathbf{x}) G^0(\mathbf{x}, \mathbf{r}; z) \right] \\ &+ \int_{-i\infty}^{+i\infty} \frac{dz}{2\pi i} \text{Tr} \left[\int d\mathbf{x} \gamma^0 G^0(\mathbf{r}, \mathbf{x}; z) g_\sigma \sigma(\mathbf{x}) G^0(\mathbf{x}, \mathbf{r}; z) \right] + \text{higher order}, \end{aligned} \quad (13)$$

where G^0 denotes the Green function for the free Dirac equation. This expansion allows us to write the vacuum polarization as a sum of infinite terms, as shown in Fig. 1.

We note that only the second term in the expansion, the Feynman diagram of which is depicted in Fig. 1(c), contains an essential divergence of the ω -meson self-energy type. This situation is the same as the vacuum polarization for the electron-positron field in QED, except for the facts that the propagating particle is massive and the diagrams including not only vector mesons but also scalar mesons contribute to the correction for the baryon density. According to Wichmann and Kroll [17], the one-loop vacuum correction may be obtained by the sum of the finite part of Fig. 1(c) and Fig. 1(a) subtracted by Fig. 1(c). Thus, the renormalized baryon density from vacuum, $\rho_{\omega \text{ ren}}^{VP}(\mathbf{r})$, is written as

$$\rho_{\omega \text{ ren}}^{VP}(\mathbf{r}) = \rho_{\omega \text{ ren}}^{(1)}(\mathbf{r}) + \rho_{\omega}^{(R)}(\mathbf{r}), \quad (14)$$

where $\rho_{\omega \text{ ren}}^{(1)}(\mathbf{r})$, which corresponds to the Uehling term [18] in QED, denotes the finite contribution from Fig. 1(c) and can be calculated from the renormalized result in the momentum representation. Choosing the renormalization point at $q^2=0$, only a wave function counterterm ζ_ω is needed to obtain the finite result:

$$\begin{aligned} \rho_{\omega \text{ ren}}^{(1)}(\mathbf{r}) &= \int \frac{d\mathbf{p}}{(2\pi)^3} e^{i\mathbf{p}\cdot\mathbf{r}} \omega_0(\mathbf{p}) \frac{g_\omega}{\pi^2} |\mathbf{p}|^2 \int_0^1 dx x(1-x) \\ &\times \ln \left(1 + \frac{|\mathbf{p}|^2 x(1-x)}{m_N^2} \right), \end{aligned} \quad (15)$$

where $\omega_0(\mathbf{p})$ is the Fourier transform of the ω -meson field $\omega_0(\mathbf{r})$. We estimate the contribution from the lowest order of g_ω^2 by this explicit expression numerically. The second term of Eq. (14), which corresponds to the Wichmann-Kroll term

[17] in QED, is the residual finite density expressed by

$$\begin{aligned} \rho_{\omega}^{(R)}(\mathbf{r}) &= \rho_{\omega}^{VP}(\mathbf{r}) - \rho_{\omega}^{(1)}(\mathbf{r}) \\ &= \int_{-i\infty}^{+i\infty} \frac{dz}{2\pi i} \text{Tr}[\gamma^0 G_V^H(\mathbf{r}, \mathbf{r}; z)] - \int_{-i\infty}^{+i\infty} \frac{dz}{2\pi i} \\ &\times \text{Tr} \left[\int d\mathbf{x} \gamma^0 G^0(\mathbf{r}, \mathbf{x}; z) g_\omega \gamma^0 \omega(\mathbf{x}) G^0(\mathbf{x}, \mathbf{r}; z) \right]. \end{aligned} \quad (16)$$

In the present work, we evaluate the vacuum correction for the baryon density by using this expression directly. After the partial-wave expansion in the Dirac angular-momentum quantum number κ , each $|\kappa|$ contribution of Eq. (16) is still finite. The partial-wave Green function of the RHA calculated numerically on the imaginary axis is used in the first term, while the analytical form of the partial-wave Green function of the free Dirac equation is used in the second term.

There are several advantages to the method of solving the Green function on imaginary axis. For example, we can carry

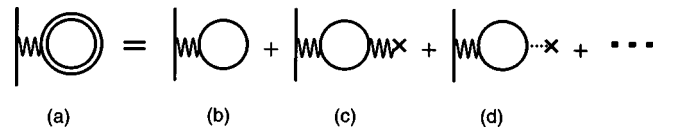


FIG. 1. Graphical representation of the baryon density in the self-consistent relativistic Hartree approximation. The double and single lines denote the Hartree propagator and the free propagator of the nucleon, respectively. The wavy and dotted lines with cross represent the vector and scalar potentials given by the previous step of the Hartree iteration, respectively. The divergence contained in (a) is caused by the contribution from (c).

out the integration over z without bothering with the poles. In addition, we can employ Gaussian quadrature for the radial integral in the second term of the right-hand side of Eq. (16), as well as the integration over z , because the Green function on the imaginary axis behaves like the modified Bessel function, which is not an oscillating function. As a result, the vacuum correction can be obtained very fast and with high precision, and it is possible to perform the RHA calculation with a practical computational time.

It should be noted that, according to naive power counting, $\rho_\omega^{(R)}(\mathbf{r})$ contains a superficially divergent contribution with the three ω mesons attached to the baryon loop, but this contribution actually vanishes as a result of current conservation. In QED, ways of calculating this term have been discussed by many authors [13,17,19] and it is well known that this contribution vanishes if the summation over κ is restricted to a finite number of terms. In this case, the κ -tail contribution is given by the extrapolation. This conclusion is valid for the present case, since the neutral ω -meson couples to the conserved baryon current. Hence, Eq. (14), together with Eqs. (15) and (16), can be used to calculate the vacuum correction for the baryon density numerically.

C. Vacuum correction for the scalar density

Next, we consider the vacuum correction for the scalar density. The regularization procedure for the scalar density is performed by using the same concept as we did for the baryon density. One can easily see that the perturbative expansion of the Hartree vacuum correction for the scalar density, corresponding to Eq. (13) gives the Feynman diagrams depicted in Fig. 2, where the four diagrams from Fig. 2(b) to 2(e) are divergent.

The scalar density is renormalized by the counterterms $\alpha_1\sigma(\mathbf{r})+1/2\alpha_2\sigma^2(\mathbf{r})+1/3\alpha_3\sigma^3(\mathbf{r})+1/4\alpha_4\sigma^4(\mathbf{r})+1/2\zeta_\sigma\partial_\mu\sigma(\mathbf{r})\partial^\mu\sigma(\mathbf{r})$ in $\delta\mathcal{L}$. The finite part of Fig. 2(c) is calculated from the renormalized result in the vacuum. The mass (α_2) and wave function (ζ_σ) counterterms are required to make the contribution finite. The result is then given by

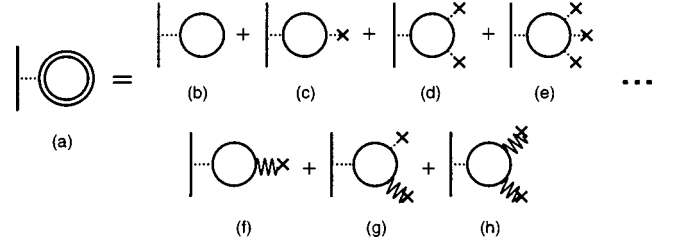


FIG. 2. Graphical representation of the scalar density in the self-consistent relativistic Hartree approximation. The same notation as in Fig. 1 is used. The divergence contained in (a) is caused by the contributions from (b) to (e).

$$\rho_{\sigma \text{ ren}}^{(1)}(\mathbf{r}) = \int \frac{d\mathbf{p}}{(2\pi)^3} e^{i\mathbf{p}\cdot\mathbf{r}} \sigma(\mathbf{p}) \frac{3g_\sigma^2}{2\pi^2} \left[\frac{1}{6} |\mathbf{p}|^2 - \int_0^1 dx (m_N^2 + |\mathbf{p}|^2 x(1-x)) \ln \left(1 + \frac{|\mathbf{p}|^2 x(1-x)}{m_N^2} \right) \right], \quad (17)$$

where $\sigma(\mathbf{p})$ is the Fourier transform of $\sigma(\mathbf{r})$ and we have chosen $q^2=0$ for the renormalization point. The physical vacuum contribution for the scalar density is given by the sum of $\rho_{\sigma \text{ ren}}^{(1)}(\mathbf{r})$ and the residual finite density denoted by $\rho_\sigma^{(R)}(\mathbf{r})$:

$$\rho_{\sigma \text{ ren}}^{VP}(\mathbf{r}) = \rho_{\sigma \text{ ren}}^{(1)}(\mathbf{r}) + \rho_\sigma^{(R)}(\mathbf{r}), \quad (18)$$

where the residual finite density $\rho_\sigma^{(R)}(\mathbf{r})$ includes the finite contributions arising from Figs. 2(b), 2(d), and 2(e). The finite residual vacuum density $\rho_\sigma^{(R)}(\mathbf{r})$ is evaluated by subtracting the contribution of Fig. 2(c) and the counterterms from the unrenormalized divergent scalar density:

$$\begin{aligned} \rho_\sigma^{(R)}(\mathbf{r}) = & \int_{-i\infty}^{+i\infty} \frac{dz}{2\pi i} \text{Tr}[G_V^H(\mathbf{r}, \mathbf{r}; z)] \\ & - \int_{-i\infty}^{+i\infty} \frac{dz}{2\pi i} \text{Tr} \left[\int d\mathbf{x} G^0(\mathbf{r}, \mathbf{x}; z) g_\sigma \sigma(\mathbf{x}) G^0(\mathbf{x}, \mathbf{r}; z) \right] \\ & - (\alpha_1 + \alpha_3 \sigma^2(\mathbf{r}) + \alpha_4 \sigma^3(\mathbf{r})) / g_\sigma, \end{aligned} \quad (19)$$

where the coefficients α_1 , α_3 , and α_4 of the counterterms are given by

$$\alpha_1 = g_\sigma \int_{-i\infty}^{+i\infty} \frac{dz}{2\pi i} \text{Tr}[G^0(\mathbf{r}, \mathbf{r}; z)], \quad (20)$$

$$\alpha_3 = g_\sigma^3 \int_{-i\infty}^{+i\infty} \frac{dz}{2\pi i} \text{Tr} \left[\int d\mathbf{x}_1 d\mathbf{x}_2 G^0(\mathbf{r}, \mathbf{x}_1; z) G^0(\mathbf{x}_1, \mathbf{x}_2; z) G^0(\mathbf{x}_2, \mathbf{r}; z) \right], \quad (21)$$

$$\alpha_4 = g_\sigma^4 \int_{-i\infty}^{+i\infty} \frac{dz}{2\pi i} \text{Tr} \left[\int d\mathbf{x}_1 d\mathbf{x}_2 d\mathbf{x}_3 G^0(\mathbf{r}, \mathbf{x}_1; z) G^0(\mathbf{x}_1, \mathbf{x}_2; z) G^0(\mathbf{x}_2, \mathbf{x}_3; z) G^0(\mathbf{x}_3, \mathbf{r}; z) \right]. \quad (22)$$

We note that α_1 , α_3 , and α_4 are independent of r , though it is still present in the right-hand side of these expressions. Performing the partial-wave expansion in free Green functions, however, each $|\kappa|$ contribution to the coefficients depends on the radial part r . With these partial-wave subtraction terms, the scalar density is calculated for each $|\kappa|$. The net effect of the scalar density generated from the vacuum polarization is obtained by taking the extrapolation $|\kappa_{\max}| \rightarrow \infty$.

III. COMPUTATIONAL DETAILS FOR THE VACUUM CORRECTION

As has been explained in the previous section, the $\rho_{\omega \text{ ren}}^{(1)}$ and $\rho_{\sigma \text{ ren}}^{(1)}$ contributions are calculated from the explicit forms (15) and (17). They contribute by a small amount as discussed below. Therefore, we explain here mainly the estimation of the residual contributions defined by Eqs. (16) and (19). We write the radial part of the residual baryon and scalar densities as

$$\rho_{\omega \text{ ren}}^R(r) = \sum_{|\kappa|=1}^{|\kappa_{\max}|} \rho_{\omega \text{ ren},|\kappa|}^R(r) \quad (23)$$

and

$$\rho_{\sigma \text{ ren}}^R(r) = \sum_{|\kappa|=1}^{|\kappa_{\max}|} \rho_{\sigma \text{ ren},|\kappa|}^R(r), \quad (24)$$

respectively. Here, $\rho_{\omega \text{ ren},|\kappa|}^R$ ($\rho_{\sigma \text{ ren},|\kappa|}^R$) represents the contribution from $|\kappa| = \pm \kappa$ to net residual baryon (scalar) density. We compute $\rho_{\omega \text{ ren},|\kappa|}^R$ and $\rho_{\sigma \text{ ren},|\kappa|}^R$ using the angular momentum decomposed form of Eqs. (16) and (19). The details of our calculation follow here. For the respective contributions of $|\kappa|$ in Eqs. (16) and (19), we carry out the integral over iz using Gaussian quadrature. The radial Green functions with imaginary energy are given in terms of the two solutions of the Dirac equation: the one regular at $r=0$ and the one regular for $r \rightarrow \infty$. Several values for the upper and lower limits of the integral over z are selected, depending on the radius parameter r around $20i-50i$ GeV. The vacuum densities $\rho_{\omega \text{ ren},|\kappa|}^R(r)$ and $\rho_{\sigma \text{ ren},|\kappa|}^R(r)$ for $z_{\max} \rightarrow \infty$ are extrapolated from the resulting integrated values. Subsequently, the sum over $|\kappa|$ is performed up to the cutoff $|\kappa_{\max}|$. This sum over $|\kappa|$ does not converge very rapidly. In the present work, $|\kappa_{\max}|$ for the baryon density is 33 for both of ^{16}O and ^{40}Ca , while $|\kappa_{\max}|$ for the scalar density is 36 for ^{16}O and 48 for ^{40}Ca . Finally, we have extrapolated the $|\kappa|$ contribution to larger values to obtain the convergent vacuum densities. As an example, the contributions from $|\kappa|=5, 10, 15, 20, 25$, and 30 for in ^{16}O are shown in Fig. 3.

An accuracy test for the computed vacuum correction of the baryon density $\rho_{\omega \text{ ren}}^R(r)$ is provided by the requirement that the total induced vacuum correction should vanish due to the conservation of baryon density,

$$\Delta B = 4\pi \int_0^\infty dr r^2 \rho_{\omega \text{ ren}}^R(r) = 0. \quad (25)$$

In the present calculation, with various QHD parameters, we found $\Delta B \sim 10^{-3}$ as a typical value for both ^{16}O and ^{40}Ca .

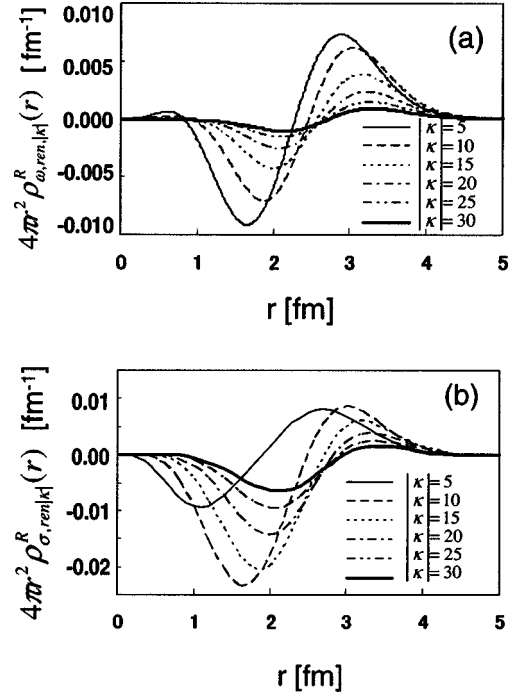


FIG. 3. The contributions from $|\kappa|=5, 10, 15, 20, 25$, and 30 to (a) the baryon density $\rho_{\omega \text{ ren},|\kappa|}^R(r)$ and (b) the scalar density $\rho_{\sigma \text{ ren},|\kappa|}^R(r)$.

For the scalar density, on the other hand, there are no constraints from conservation laws. However, it would be reasonable to expect the numerical error in the scalar density to be of the same order of magnitude as the one in the baryon density.

In Sec. II B, we mentioned that the divergence of the unrenormalized baryon density in the present model has the same structure as the unrenormalized vacuum charge density of the electron-positron field in the QED correction. However, the dependence on the partial-wave contribution is largely different from that for the QED case: a large $|\kappa_{\max}|$ is required to achieve the convergence as seen in Fig. 3, while for the renormalized charge density in QED the term with $|\kappa_{\max}|=1$ gives a good approximation [13]. In addition, it should be pointed out that Eqs. (15) and (17) are negligible for the present calculation, i.e., $\rho_{\omega \text{ ren}}^{(1)}$ and $\rho_{\sigma \text{ ren}}^{(1)}$ are an order of magnitude smaller than the residual densities. This stands in contrast with the QED calculation, in which the corresponding contribution, known as the Uehling effect, has a dominant contribution [19]. These differences from QED seem to be caused by the ω - σ couplings as well as the large coupling constant of the nuclear force. In particular, the baryon density, the source of the ω meson, is strongly influenced by the σ meson. This is shown in Fig. 4, where the baryon densities $\rho_{\omega \text{ ren}}^{(1)}(r)$ with and without σ meson are compared; it is clear from that graph that the vacuum correction for the baryon density is negligibly small if only the ω meson is taken into account. We found that the baryon density induced by the vacuum polarization comes from diagrams with σ -meson self-energy insertions mainly.

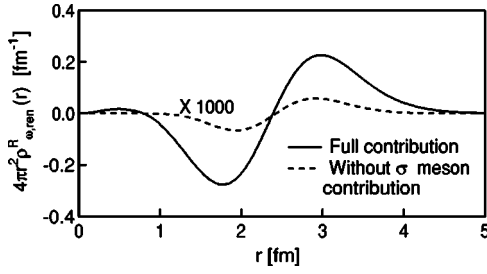


FIG. 4. Comparison between the baryon densities with and without the σ -meson contribution. The latter is given by solving the Dirac Green function with the ω -meson field only.

IV. RESULTS AND DISCUSSION

Here, we show the results of the relativistic Hartree calculation with a rigorous treatment of renormalized densities in ^{16}O and ^{40}Ca , based on the Lagrangian density of Eq. (1). The numerical procedure of the present RHA calculation is similar to that used in the conventional RMF calculation; firstly, the Dirac equation (3) is solved under the external ω and σ fields, for the valence nucleons only. Secondly, using the same potential, we calculate the vacuum densities by means of the Green function described in the previous section. Thirdly, the equations of motion of mesons, Eqs. (6) and (7), are solved with the source terms due to the valence nucleons and vacuum contributions. Substituting these results in the Dirac equation, we complete one iteration step. Using the same method as indicated in the previous section, the energy shift due to the vacuum polarization is estimated by

$$E_{VP} = \int d\mathbf{r} \left[\int_{-i\infty}^{+i\infty} \frac{dz}{2\pi i} \text{Tr}[\gamma^0 (G_V^H(\mathbf{r}, \mathbf{r}; z) - G^0(\mathbf{r}, \mathbf{r}; z))]z + (CT) \right], \quad (26)$$

$$CT = -1/4\zeta_\omega(\nabla\omega_0)^2 + 1/2\zeta_\sigma(\nabla\sigma)^2 + \alpha_1\sigma + 1/2\alpha_2\sigma^2 + 1/3\alpha_3\sigma^3 + 1/4\alpha_4\sigma^4, \quad (27)$$

which is calculated at each iteration. The iteration is continued until the total binding energy of the nucleus $E_{\text{total}} = E_{\text{meson}} + E_{\text{valence}} + E_{VP}$ converges, showing self-consistency.

The QHD parameter set is chosen so as to reproduce reasonably well the experimental values of the total binding energies, the rms radii, and the single-particle energies for both of ^{16}O and ^{40}Ca . In the second column of Table I, we give the results with the coupling constants and masses $g_\sigma = 7.38$, $g_2 = 7.90$, $g_3 = 3.20$, and $m_\sigma = 458.0$ MeV for the σ meson, and $g_\omega = 9.18$ and $m_\omega = 783.0$ MeV for the ω meson. The results of the RMF calculation with the parameter set TM2 [20] and experimental data taken from Ref. [21] are also shown in the third and last columns, respectively. We see that our total binding energies including the vacuum correction and rms radii are similar to those of RMF and agree with the experimental data well.

The vacuum contribution plays a crucial role for the generation of the weak meson fields. In Fig. 5, we plot the

σ -meson field in nuclear matter as a function of the coupling constant g_σ while keeping the other parameters fixed. The figure shows that the vacuum correction contributes destructively to the valence contribution, and it is impossible to obtain a strong meson field unless a very large coupling constant is used. We could of course choose such a parameter set with large coupling constants. However, this would have produced an unstable solution in the RHA calculation, since the deeply-bound antinucleon states produced by the strong ω and σ fields with large coupling constants, imply to produce a large vacuum effect, which works in the opposite direction. Such a RHA solution is not realistic, because it is unstable even for trivial fluctuations in the nucleon density. Hence, we have to choose a parameter set which produces a weak field in the self-consistent iteration.

The RMF reproduces the observed tendency of the single-particle spectra reasonably well, due to the small effective mass of the nucleon, $m_N^*(r) = m_N + g_\sigma\sigma(r)$. The fact that the scalar field is suppressed in the RHA results in the large effective mass. As a result, it raises a problem in fitting the single-particle energies. As seen in Table I, the energy splittings in the single-particle states of the present RHA are very small, and they are unlikely to agree with the experimental values. This is a known problem, from previous RHA calculations, using the local-density approximation and the derivative expansion to estimate the vacuum correction [8,11]. It is difficult to resolve this problem in the RHA with the ordinary QHD models, used up to now.

Thus the QHD models require a mechanism for producing the spin-orbit splittings, other than the small effective mass. One suggestion is made in Refs. [12,23], where a tensor-coupling of the ω meson is introduced in order to provide the spin-orbit splittings. However, the ω -meson coupling with the nucleon is known to be dominated by the vector coupling in the nucleon-nucleon potential. Another candidate to solve this problem may be the possibility of the finite pion mean field in the relativistic Hartree framework, which was suggested to provide the spin up and spin down partners with large energy separations [22]. It is interesting to extend the present RHA calculation by taking these effects into account. This is certainly a subject to be worked out in a future study.

V. COMPARISON WITH THE PREVIOUS METHOD FOR THE VACUUM POLARIZATION

The effect of the negative-energy nucleons for finite nuclei was first estimated by the local-density approximation [5,7,9]. It was developed further by applying the derivative-expansion method [6,8,11,12]. In this section, we compare our resulting densities, induced by the vacuum polarization, with those of the local-density approximation and the derivative-expansion method. The local-density approximation uses as input results from the calculations of the infinite nuclear matter. In this approximation, the vacuum correction is given by

$$\rho_{\sigma,ren}^{VP(LDA)}(r) = -\frac{1}{\pi^2} [m_N^*(r)\ln(m_N^*(r)/m_N) + 1/3m_N^3 - 3/2m_N^2m_N^*(r) + 3m_Nm_N^*(r) - 11/6m_N^3(r)], \quad (28)$$

and the scalar density decreases in the nuclear interior. The

TABLE I. The total binding energies, the rms charge radii, and the single-particle energies in ^{16}O and ^{40}Ca .

| | Present RHA | TM2 | Experiment |
|--------------------------------------|-------------|---------|-------------|
| ^{16}O | | | |
| $E_{\text{total}}/A(E_{VP}/A)$ (MeV) | 8.05(1.69) | 7.93(-) | 7.98(-) |
| r_{ch} (fm) | 2.65 | 2.67 | 2.74 |
| Single particle state of proton | | | |
| $1s_{1/2}$ (MeV) | 31.0 | 38.2 | 40 ± 8 |
| $1p_{3/2}$ (MeV) | 15.6 | 18.6 | 18.4 |
| $1p_{1/2}$ (MeV) | 13.3 | 11.1 | 12.1 |
| Single particle state of neutron | | | |
| $1s_{1/2}$ (MeV) | 35.6 | 42.3 | 45.7 |
| $1p_{3/2}$ (MeV) | 19.7 | 22.4 | 21.8 |
| $1p_{1/2}$ (MeV) | 17.4 | 14.8 | 15.7 |
| ^{40}Ca | | | |
| $E_{\text{total}}/A(E_{VP}/A)$ (MeV) | 8.47(2.23) | 8.48(-) | 8.55(-) |
| r_{ch} (fm) | 3.42 | 3.50 | 3.45 |
| Single particle state of proton | | | |
| $1s_{1/2}$ (MeV) | 36.5 | 45.2 | 50 ± 11 |
| $1p_{3/2}$ (MeV) | 25.5 | 30.7 | |
| $1p_{1/2}$ (MeV) | 24.0 | 36.2 | 34 ± 6 |
| $1d_{5/2}$ (MeV) | 13.5 | 16.1 | |
| $1d_{3/2}$ (MeV) | 11.0 | 8.7 | 8.3 |
| $2s_{1/2}$ (MeV) | 9.1 | 8.5 | 10.9 |
| Single particle state of neutron | | | |
| $1s_{1/2}$ (MeV) | 45.5 | 53.1 | |
| $1p_{3/2}$ (MeV) | 33.8 | 38.3 | |
| $1p_{1/2}$ (MeV) | 32.3 | 33.8 | |
| $1d_{5/2}$ (MeV) | 21.2 | 23.4 | |
| $1d_{3/2}$ (MeV) | 18.7 | 15.9 | 15.6 |
| $2s_{1/2}$ (MeV) | 16.9 | 15.6 | 18.1 |

vacuum does not change the baryon density, because of the conservation of the baryon number. In the derivative-expansion method, on the other hand, the presence of the derivative term allows a nonvanishing correction for the baryon density, as well as for the scalar density:

$$\rho_{\omega, \text{ren}}^{VP(DE)}(r) = -\frac{g_{\omega}}{3\pi^2} \nabla \cdot \ln\left(\frac{m_N^*(r)}{m_N}\right) \nabla \omega_0(r), \quad (29)$$

$$\begin{aligned} \rho_{\sigma, \text{ren}}^{VP(DE)}(r) = & \rho_{\sigma, \text{ren}}^{VP(LDA)}(r) - \frac{g_{\sigma}}{2\pi^2} \nabla \cdot \ln\left(\frac{m_N^*(r)}{m_N}\right) \nabla \sigma(r) \\ & - \frac{g_{\sigma}^2}{4\pi^2 m_N^*(r)} (\nabla \sigma(r))^2 + \frac{g_{\omega}^2}{6\pi^2 m_N^*(r)} (\nabla \omega(r))^2, \end{aligned} \quad (30)$$

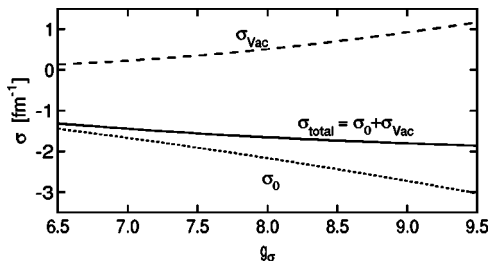


FIG. 5. The scalar potential in nuclear matter. A σ -meson mass $m_{\sigma}=458.0$ and a Fermi momentum $k_F=1.42$ are employed. σ_0 denotes the ordinary σ -meson field, generated from the valence nucleons while σ_{vac} denotes the contribution from the vacuum. Due to the cancellation between them, the net σ -meson field does not increase smoothly with the coupling constant, g_{σ} .

where only the leading order of the derivative terms is taken into account. The baryon and scalar densities induced by the vacuum polarization are given in Fig. 6, together with those from the local-density approximation and the derivative expansion. There, for purpose of comparison, we assume the same potential in evaluating the vacuum polarization. We can see that the densities obtained by the local-density approximation are corrected significantly, not only for the baryon density, which vanishes in this approximation, but also for the scalar density. Both the scalar and baryon density profiles

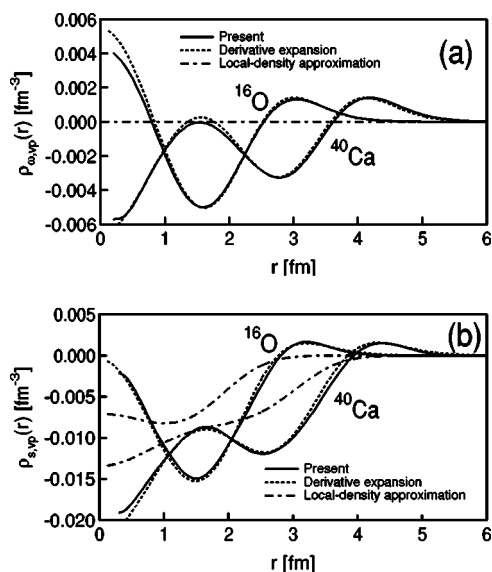


FIG. 6. The vacuum correction for (a) baryon and (b) scalar densities.

obtained by the present calculation are in a surprisingly good agreement with those of the derivative expansion.

However, this cannot always be the case [16], and the excellent agreement between our method and the leading-order derivative expansion can be attributed to the specifics of the σ - ω model. Consider, for example, the vacuum correction in the baryon density without σ meson. Using the present method, the vacuum correction in this situation can turn out to be significant with a large coupling constant of the ω meson. As found in Eq. (29), on the other hand, the vacuum correction from the derivative expansion vanishes exactly for $m_N^*(r) \rightarrow m_N$. Hence, we find that σ meson plays an important role in the agreement between our method and the leading-order derivative expansion. Thus the present calculation supports that the leading-order derivative expansion is greatly useful for the estimation of the vacuum correction in the RHA.

In the present calculation of the full RHA for finite nuclei, the vacuum-polarization corrections (15) and (17) to the meson propagators are implicitly taken into account to all orders by the iteration method achieving the self-consistency in the relativistic Hartree approximation. There, the unphysical pole in the meson propagator at finite momentum transfer, known as the Landau ghost, may affect the present numerical results [7,24] through integration over the momentum transfer. However, this unphysical effect is not significant in the RHA of finite nuclei, because even if the (15) and (17) terms

are totally ignored in the calculation, the final results for the scalar and vector densities do not change appreciably. The good agreement with the results of the derivative expansion, where the Landau ghost plays no role, also implies that the unphysical effect is negligible.

VI. SUMMARY

We have developed a rigorous method to calculate vacuum-polarization effects in the relativistic Hartree approach. The renormalized baryon and scalar densities have been evaluated within a practical computational time by replacing the summation over the Hartree basis by the numerical integral of the Dirac Green function over the imaginary energy. We have obtained numerical results, indicating that the vacuum corrections for the baryon and scalar densities are non-negligible in the RHA calculation.

Our results, exploiting the Walecka model, have reproduced the experimental binding energies and rms radii of ^{16}O and ^{40}Ca nicely, after adjustment of the parameters. However, it was impossible to find a QHD parameter set capable of reproducing the spin-orbit splittings in accordance with the observed data and as required by the nuclear shell model. In the σ - ω model, the main attraction is caused by the large σ -mean field, which provides a small nucleon effective mass in finite nuclei. However, the negative-energy nucleons will acquire a mass differing from that of the free nucleon only reluctantly. On the whole, the effective nucleon mass remains quite large, implying that the spin-orbit splittings in the single particle spectra come out very small. The QHD type effective theory based on the σ - ω mesons, then, needs to include new types of interaction terms and/or go beyond the RHA approximation to solve this problem.

We have found that our results from the RHA calculation are very similar to those in Refs. [6,11], where the derivative-expansion method was used to estimate the vacuum polarization. In particular, it has been shown that the agreement of the density profiles of the vacuum correction is quite good. Thus the validity of this approximation has been confirmed by the present calculation.

ACKNOWLEDGMENTS

This work has been supported by MATSUO FOUNDATION, Sugunami, Tokyo. A.H. would like to thank Professor S. Kita and Professor Y. Tanaka for giving him the opportunity to do this work and Dr. A. Deuzeman for useful discussions. Y.H. acknowledges Dr. K. Tanaka for useful discussion.

- [1] J. D. Walecka, *Ann. Phys. (N.Y.)* **83**, 491 (1974); B. D. Serot and J. D. Walecka, *Adv. Nucl. Phys.* **16**, 1 (1986); B. D. Serot and J. D. Walecka, *Int. J. Mod. Phys. E* **6**, 515 (1997).
 [2] E. Klempt, F. Bradamante, A. Martin, and J. Richard, *Phys. Rep.* **368**, 119 (2002).

- [3] W. Greiner, *Heavy Ion Phys.* **2**, 23 (1995).
 [4] A. Haga, Y. Horikawa, Y. Tanaka, and H. Toki, *Phys. Rev. C* **69**, 044308 (2004).
 [5] C. J. Horowitz and B. D. Serot, *Phys. Lett.* **140B**, 181 (1984).
 [6] R. J. Perry, *Phys. Lett. B* **182**, 269 (1986).

- [7] S. Ichii, W. Bentz, A. Arima, and T. Suzuki, Nucl. Phys. **A487**, 493 (1988).
- [8] D. A. Wasson, Phys. Lett. B **210**, 41 (1988).
- [9] W. R. Fox, Nucl. Phys. **A495**, 463 (1989).
- [10] R. J. Furnstahl and C. E. Price, Phys. Rev. C **40**, 1398 (1989); **41**, 1792 (1990).
- [11] G. Mao, H. Stöcker, and W. Greiner, Int. J. Mod. Phys. E **8**, 389 (1999).
- [12] G. Mao, Phys. Rev. C **67**, 044318 (2003).
- [13] M. Gyulassy, Phys. Rev. Lett. **33**, 921 (1974); **32**, 1393 (1974); Nucl. Phys. **A244**, 497 (1975).
- [14] G. Soff and P. J. Mohr, Phys. Rev. A **38**, 5066 (1988).
- [15] P. G. Blunden, Phys. Rev. C **41**, 1851 (1990).
- [16] I. W. Stewart and P. G. Blunden, Phys. Rev. D **55**, 3742 (1997).
- [17] E. H. Wichmann and N. M. Kroll, Phys. Rev. **101**, 843 (1956).
- [18] E. A. Uehling, Phys. Rev. **48**, 55 (1935).
- [19] G. A. Rinker, Jr. and L. Wilets, Phys. Rev. A **12**, 748 (1975).
- [20] Y. Sugahara and H. Toki, Nucl. Phys. **A579**, 557 (1994).
- [21] J. H. E. Mattauch, W. Thiele, and A. H. Wapstra, Nucl. Phys. **67**, 1 (1965); J. W. Negele, Phys. Rev. C **1**, 1260 (1970); D. Vautherin and D. M. Brink, *ibid.* **5**, 626 (1972); H. de Vries, C. W. de Jager, and C. de Vries, At. Data Nucl. Data Tables **36**, 495 (1987).
- [22] Y. Ogawa, H. Toki, S. Tamenaga, H. Shen, A. Hosaka, S. Sugimoto, and K. Ikeda, Prog. Theor. Phys. **111**, 75 (2004).
- [23] Y. Sugahara and H. Toki, Prog. Theor. Phys. **92**, 803 (1994).
- [24] K. Tanaka, W. Bentz, A. Arima, and F. Beck, Nucl. Phys. **A528**, 676 (1991).